An innovative non-destructive approach for the shrinkage assessment in two-component grout application

Tunnelling and Underground Space Technology 159 (2025) 106424

Contents lists available at ScienceDirect

Tunnelling and Underground Space Technology incorporating Trenchless Technology Research

journal homepage: www.elsevier.com/locate/tust

An innovative non-destructive approach for the shrinkage assessment in two-component grout application

Aarathy Ezhuthupally Reghuprasad, Carmine Todaro *, Francesca Pace, Daniele Peila, Alberto Godio

DIATI, Department of Environment, Land and Infrastructure Engineering, Politecnico di Torino, Corso Duca degli Abruzzi 24, 10129 Torino (TO), Italy

ARTICLE INFO

Keywords:
Two-component grout
Shrinkage
Fiber Bragg Grating
Backfilling

ABSTRACT

In this study, a well-known technology known as the Fiber Bragg Grating (FBG) has been employed for the first time for the study of the two-component grout (2CG), the most used material for the backfilling phase in mechanised tunnelling. Using FBG, it has been possible to monitor both the temperature and the shrinkage of the 2CG since the first moments after the gelation of the grout. The procedure proposed and the outcomes presented in terms of shrinkage put alight the validity of the proposed approach, and the crucial importance of the curing environment. For a fixed mix design, values of shrinkage lower than 500 με have been founded after 16 days of curing in water irrespective of the tested bentonite, while in dry environment the shrinkage reached values higher than 3000 με.

1. Introduction

Static monitoring is an early assessment method that can offer a preliminary assessment of the condition of the structure. It involves the continuous or periodic measurement and analysis of various parameters characterizing the behaviour and condition of deformation, like accessing the integrity of the structure, performance, and safety of a building, dam, tunnel, bridge, or any kinds of infrastructure.

The main advantages of static monitoring are the early detection of structural issues, identification of potential risks, implementation of the appropriate maintenance and repair. This is mainly done by using the sensors, instruments, and data acquisition system for collecting those data related to parameters such as deformation, stress, strain, displacement, and temperature. The most commonly used sensors are strain gauges, displacement transducers, temperature sensors, tiltmeters, and fiber optic sensors.

The static monitoring of tunnels at an early age by measuring the temperature and shrinkage using fiber optic sensors is carried out to analyse the behaviour and performance of the tunnel linings during the construction and operative phases. As we know, shrinkage is a time-dependent deformation that occurs in all types of concrete. This happens mainly due to the loss of water during the curing phase (Kim and Lee, 1998). Early age shrinkage and temperature monitoring is important as it helps to understand the excessive shrinkage, and thermal gradients that can lead to cracking in the construction phase, thus allowing the optimization of the cement material, the mix design and the water/cement ratio used for the construction process.

Shield machines used for tunnel excavation have increasingly been used mainly for metro and underwater tunnels due to their faster construction speed and lower influence on ground disturbance than the traditional tunneling methods (He et al., 2020). During the Tunnel Boring Machine shield (TBM) advancements, a void, commonly called “annulus” is created behind the shield tail. The creation of this gap cannot be avoided since it is due to the difference in diameter between the lining extrados and the shield inner diameter. The dimension of this gap has a centimetric order of magnitude (Thewes and Budach, 2009) and the filling of this annulus is a crucial operation in the mechanized tunneling excavation process called backfilling. So special care is required during this backfilling phase for shielded machines, irrespective of their excavation system (rock TBM, slurry, Earth Pressure Balance or variable density). The backfilling phase prevents or minimizes the surface settlements thereby ensuring a homogenous, uniform, and immediate contact between the ground and lining, waterproofing of the tunnel, and the gasketry.

To achieve an efficient backfilling, the material used for injection should guarantee the following performance, technical, and operational characteristics (Todaro et al., 2022):

* Corresponding author.
E-mail address: carmine.todaro@polito.it (C. Todaro).

https://doi.org/10.1016/j.tust.2025.106424
Received 12 June 2024; Received in revised form 16 January 2025; Accepted 20 January 2025
Available online 27 February 2025

- quite instantaneous gelation of the material injected, to avoid surface settlements or linings' moving during the TBM advancements;
- the annulus must be consistently and entirely filled for the linings to be connected to the surrounding ground on a regular basic, regarding the mix's transportability, the system's dependability must be ensured. Therefore, the grout must be designed to prevent clogging of the injection pipes, as well as segregation and bleeding of the pumps in relation to the amount of time the grout is transported, as well as the distance from batching to injection;
- regarding its physical properties and mechanical behavior, the material should be homogeneous across the annulus, furthermore it should satisfy the construction site's technical specification;
- the injected material should resist against the action of groundwater.

Among the existing alternative materials for backfilling in tunneling applications, the two-component grout (2CG) is the most widely used because of its optimal capability to control surface settlements in the short term and its fast hardening (Peila et al., 2011). It is typically a super fluid grout whose workability is guaranteed for a long duration from batching to transport and injection. During the injection at the annulus, an accelerator admixture is added, only a few centimetres before the exit hole of the nozzle. This mix begins to gel after the accelerator is added in a short time — typically 8 to 12 s —during which the TBM moves forward by about 10 to 20 mm. This gel immediately begins to develop mechanical strength (Oggeri et al., 2021; Oreste et al., 2021).

The 2CG is obtained by mixing two fluids, that in jargon are called component A and component B. Component A is a cementitious mix made up of water, cement, bentonite, and retarding /fluidifying agent. Component B is an accelerator agent (commonly a sodium silicate solution) (Song et al., 2020; Di Giulio et al., 2023). The hardened mix's homogeneity formed after gel formation is greatly improved by the bentonites. This ingredient also helps to reduce the bleeding, plays an active role in the strength at short terms, provides better impermeability to the system by assisting in the gelling process when the flow pauses because the annulus is full and in establishing the thixotropic consistency (Sharghi et al., 2018; Todaro et al., 2023). The retarding agent prevents the mix from setting thereby ensuring its usability for up to 72 h after the batching (Youn et al., 2016). A rapid gel formation results from the addition of the accelerator admixture to the component A.

Various research studies have been done on the role of each ingredient in the 2CG during the past decades. Dal Negro et al. (2014) explained how the retarding agent ensures the necessary workability. Mesboua et al. (2018) put forward the role of bentonite in the stability of the component A. Moreover, the waterproofing capacity of the hardened grout and the gelation phase confirmed the influence of bentonite by Peila et al. (2011), who investigated on the right choice and dosage of the bentonite. Recently, Todaro and Pace (2022) studied the role of bentonite in the two component grout applications with a specific focus on the elastic properties at a short curing time. However, the material is not yet well known and one of the main lacks is related to the strain. It is practically impossible to measure the early age strain of the 2CG in the initial hours after casting since strain or displacement gauges cannot be attached until a minimum strength is developed. However, the assessment of the shrinkage for the 2CG has become important in the last years: currently, the technical specifications of construction site often require the assessment of the shrinkage (Todaro et al., 2022; Càmara, 2018). This innovative demand focused on the shrinkage of the 2CG comes from tunnelling designers that are starting to characterise all the material involved in a tunnelling construction in increasingly more detail. Specifically, for the 2CG, the need for an accurate knowledge of the potential surface subsidence or lining movements is crucial for a successful tunnel construction. If on the one side the elastic characterisation (Young modulus, shear modulus, Poisson's ratio) (Todaro et al., 2020a) provides information related to strains due to an applied load, for the shrinkage the phenomenon is more complex than the elastic behaviour. Shrinkage indeed causes strains that are physiologically linked to the material, being the 2CG a cement-base material. However, at the state of the art, information related to the evolution in time of the shrinkage and its dependence from the mix-design or the curing environment is very poor. Based on the authors' experience, it is known from the "concrete world" that curing in aggressive waters (for instance sulphate waters) could cause strong expansion (and consequent destruction) of the grout: a laboratory test campaign focused on the shrinkage assessment could consequently lead to optimise the mix design selecting specific cement or additives.

Various studies have been done on the estimation of physical properties of the concrete using different technologies. Slowik et al. (2004) and later Wong et al. (2007) investigated the simultaneous measurement of early age shrinkage and temperature of the cement using Fiber Bragg Grating (FBG) sensors. A new approach based on FBG sensors and the intrinsic advantages was studied by Luo et al. (2013), expressly for the early age analysis. A multipoint approach of measurement of early age properties was later conducted by Pei et al. (2014). These works have only focused on the early age measurement of the standard cement paste.

Clearly stated the importance of the shrinkage assessment for tunnelling stockholders, the goal of this paper is to have a better understanding of the 2CG by using FBG, a relatively recent technology. The shrinkage and temperature variations of 2CG using FBG sensors have been studied. After preparing special casting moulds, the sensors have been embedded inside the specimens of the 2CG. Four different bentonites have been used for preparing the 2CG mixes, while the dosages of the other ingredients were always the same. Then, the early age shrinkage and temperature measurement of the 4 grouts were carried out. Thanks to the fixed mix-design and the fixed dosages in terms of kg of ingredient for 1 m^3 of 2CG, the obtained trends in terms of shrinkage and temperature were similar. Consequently, a preliminary statistical analysis was performed on these outcomes trying to recognise the key parameters (hereinafter called "characteristic values") useful to describe the charts and the phenomena.

It should be highlighted that the proposed technology and approach are intended to provide an innovative method for providing answers for the assessment of the shrinkage of the 2CG. This research cannot obviously cover all aspects related to the FBG applications to the 2CG, as well as the obtained results in terms of shrinkage (με) cannot be considered as universal. Despite this, the innovation proposed permits to overcome the limitations of the most popular standards used for assessing the shrinkage, since also the assessment at very short curing times (the most critical and investigated curing time for the backfilling) has been made possible. Furthermore, the order of magnitude of our outcomes could be surely considered as a reference value for standard 2CG cured in standard water.

2. Methodology

The early age temperature monitoring is important during the casting of concrete structures. Conventionally, temperature monitoring can be done using thermocouples with an acceptable accuracy, but the limitation is the sensing in only certain locations. The mechanical and electrical strain gauges used for measuring the shrinkage cannot be attached before the mix is hardened, hence this technique also fails to measure the early age shrinkage. There are other techniques like ultrasonic, calorimetric measurement that requires complex and delicate experimental setups. Compared to all these techniques, the FBG technology is more attractive due to the small size, ease of installing the sensor before casting, accuracy in measuring the shrinkage soon after the casting, immune to asymmetry.

It is well known one of the limitations of FBG sensors is the inability to discriminate between strain and temperature in a single measurement of the Bragg wavelength shift. To overcome this, several techniques have been proposed such as dual-wavelength superimposed gratings, long-

period gratings/hybrid Bragg gratings (Srimannarayana et al., 2008), and dual-diameter FBGs (Jiang et al., 2015).

For the investigation of the early age properties of the 2CG, the dual FBG sensors were taken into consideration for the simultaneous measurement of strain and temperature. For discriminating the temperature measurement, the dual FBG sensors were encapsulated into a capillary tube. Before casting the bare dual FBG and the encapsulated dual FBG sensors were inserted into the casting mould. They were inserted horizontally into the casting mould at a middle position horizontally and locked to the mould with a quick-setting glue.

The interrogation system used for the measurement was Micron Optics Si155 and it was used to acquire the data of FBG wavelength shift with a sampling frequency of 1 kHz. This system can potentially acquire the measurements of hundreds of sensors on four parallel and 160 nm wide optical channels.

2.1. The available standards and the strength of FBG

The first demands for the shrinkage assessment are relatively recent in the tunnelling world. In the scientific literature the first information related to construction sites that required a complete characterisation of the 2CG (also including the shrinkage assessment) is available in Todaro et al. (2022). It is reported that statistically 12 % of construction sites in last years have inserted the shrinkage assessment in the construction site standards acceptance criteria. Pertaining to the standards used for this assessment, as occurred in the past for other key parameters, the existing procedures for the standard concrete have been shifted to the 2CG world. However, relevant differences exist between the innovative procedures introduced in this work (FBG) and the actually used standard (hereafter "old standard" or OS). For this comparison analysis, the standard CEN (2002) can be considered since it is based on samples with a geometry in compliance to CEN (2016), that is the most worldwide used for mechanically characterise the 2CG. The main difference between FBG and OS is related to the first determination that can be carried out: the FBG method provides readings almost instantaneously after the casting phase. In this way, the short term, that is considered the most important phase for the backfilling (Sharghi et al., 2017), can be successfully investigated. According to OS instead, the samples need 24 h to be ready for the assessment. This time interval is mandatory since specific steel pins, embedded in the grout, should be strongly linked to the body of the sample. These 2 pins are the reference points for the subsequent measures and thanks to a high precision comparator fixed on a frame, the variation in length can be measured (Fig. 1). In conclusion, if OS is applied, the shrinkage related to the short terms is lost.

It is also a due to report that, thanks to FBG, the limitation related to "weak" two-component grouts (backfilling grout that commonly do not overcome 1.5–1.6 MPa of UCS after 28 days of curing) can be successfully overcome. When weak two-component grouts are studied, breakages of the samples commonly occur during the demoulding phase due to the poor strength of the grout and hence the pins are disconnected by the body of the sample. Small cracks sometimes occur in the contact area pin-sample without the complete ejection of the pin (not always these cracks are easily recognizable). This irreparably affects all the readings. In both cases, the shrinkage assessment with OS for weak two-component grouts often results so laborious and difficult that sometimes the test campaign fails.

To sum up, the FBG technique applied to 2CG includes two unquestionable advantages: the immediate reading of shrinkage after the casting with the possibility to study the short curing time and the possibility to assess the shrinkage even though low binder dosages are used.

2.2. Two component mix used

The used two-component mix design is reported in Table 1.

For the study of the early age shrinkage and temperature measurement, four different types of bentonites were used, according to the previous study published by Todaro and Pace (2022). Regarding the use of bentonite (characterized by slightly different unit weights) the maximum difference in the water dosage was to 10 kg/m^3. In accordance with EFNARC (2005), this variation has no impact on the water-cement ratio (w/c) since it is inside the tolerance commonly accepted in construction sites. The cement used consisted of 95 % clinker and 5 % of minor constituents, excluding calcium sulphate and additives. The mixing phase and the casting phase were performed according to Todaro

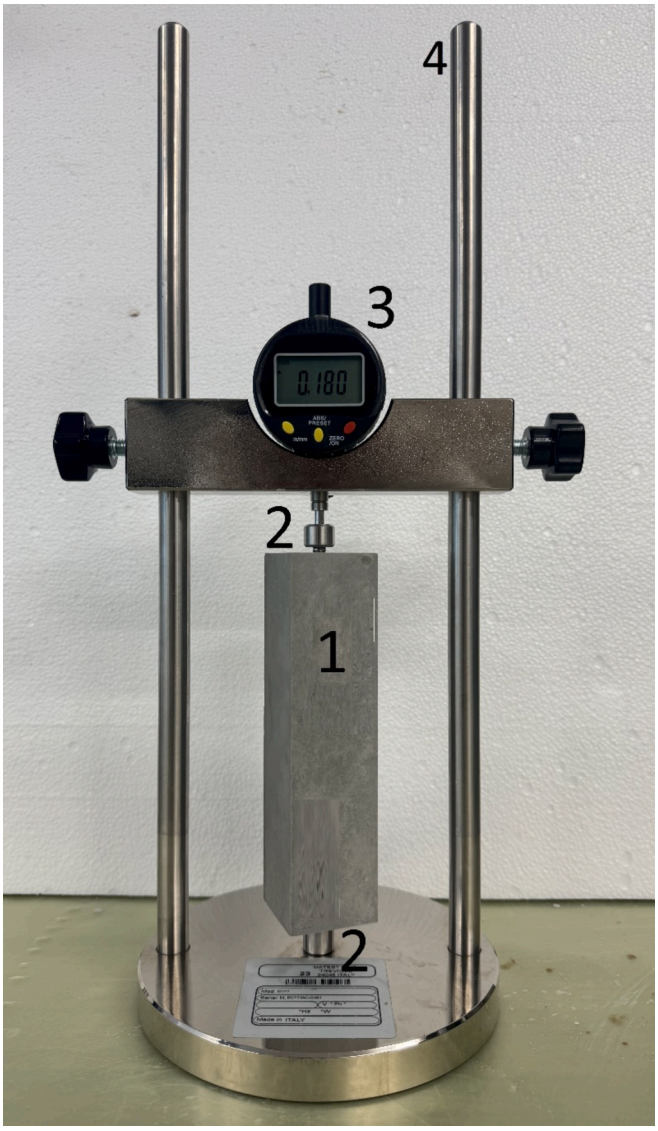

Fig. 1. Equipment for the shrinkage assessment carried out according to OS (CEN, 2002). 1. Sample body; 2. Steel pins embedded in the sample during the casting phase; 3. High precision comparator; 4. Measurement frame and support.

Table 1
Two Component grout mix design used.

	Ingredients	Dosage(kg/m^3)
Component A	Water	853
	Bentonite	30
	Portland Cement CEM I 52,5R	230
	Retarding/fluidifying agent-Mapequick CBS1	3.5
Component B	Accelerator – Mapequick CBS3	81

et al. (2020b).

Table 2 describes the name of the grouts, bentonite pictures, swell index (SWI), and smectite percentage. The swell index is a factor that describes the ability of the bentonite to swell as it interacts with water. The XRD analysis of the mix were conducted by Todaro and Pace (2022) for the estimation of percentage by weight of smectite.

2.3. Design of The FBG sensor

Since the FBG sensor is sensitive to both strain and temperature, the bragg wavelength shift can be influenced by both stress and thermal change of the grating region. For measuring the shrinkage and temperature simultaneously we needed to distinguish and separate the responses. This was achieved by using two dual FBG sensors in an identical situation with one of them being free and the other being packaged inside an encapsulated tube.

Table 2
Details of four different bentonites and relative grouts (B1-B4). Data taken from Todaro and Pace (2022).

Name of the grout	Bentonite pictures	Smectite content (% by weight)	SWI (ml/g)
B1		92	23
B2		98	13
B3		88	14
B4		72	19.7

The linear equation for these two sensors is given by:

$$\begin{aligned} \Delta\lambda_{B1}/\lambda_{B1} &= k_{\varepsilon 1}\Delta\varepsilon + k_{T1}\Delta T \\ \Delta\lambda_{B2}/\lambda_{B2} &= k_{T2}\Delta T \end{aligned} \tag{3.1}$$

where λ_B denotes the Bragg wavelength, $\Delta\lambda_B$ denotes the change of bragg wavelength, $k_\varepsilon = (1-p_e)$ and $k_T = (\alpha+\xi)$ are the strain optic and thermal optic coefficient respectively. Where $(1-p_e)$ is photo elastic parameter related to the fiber property, α and ξ are the thermal expansion coefficient and thermal optic coefficient of the fiber core, strain change Δε, and temperature change ΔT. Here the subscripts 1 and 2 represent the strain and temperature sensors, respectively. We can express Eq. (3.1) in the matrix form:

$$\begin{pmatrix} \Delta\lambda_{B1}/\lambda_{B1} \\ \Delta\lambda_{B2}/\lambda_{B2} \end{pmatrix} = \begin{pmatrix} k_{\varepsilon 1} & k_{T1} \\ 0 & k_{T2} \end{pmatrix} \begin{pmatrix} \Delta\varepsilon \\ \Delta T \end{pmatrix} = K \begin{pmatrix} \Delta\varepsilon \\ \Delta T \end{pmatrix}$$

and after determining the measurand vector on the right-hand side through the inversion of the sensitivity matrix, we obtain:

$$\begin{aligned} \Delta\varepsilon &= \frac{1}{k_{\varepsilon 1}}\left(\frac{\Delta\lambda_{B1}}{\lambda_{B1}}\right) - \frac{k_{T1}}{k_{\varepsilon 1}k_{T2}}\left(\frac{\Delta\lambda_{B2}}{\lambda_{B2}}\right) \\ \Delta T &= \frac{1}{k_{T2}}\left(\frac{\Delta\lambda_{B2}}{\lambda_{B2}}\right) \end{aligned} \tag{3.2}$$

From (3.2), we can determine the early age shrinkage (Δε) and temperature(ΔT) by considering negligible the slippage between the fiber and the mix. The temperature measurement is obtained directly from the FBG sensor inside the encapsulated tube.

2.4. Sensor calibration

Before embedding the polyimide FBG sensor into the two components mix it was necessary to calibrate the wavelength shift with the change of temperature. In the test, the calibration was done using the encapsulation of the FBG sensor in two different materials of the capillary tube (Mamidi et al., 2014). The thermal conductivity and thermal capability of the material for the capillary tube was considered while selecting the material given in Table 3. The material of the capillary tube used was borosilicate glass and stainless steel. Both the tubes were 20 cm long, with an outer diameter of 1 mm and inner diameter of 0.5 mm. Fig. 2 shows the apparatus and modality for the sensor calibration particularly for the temperature measurement.

The bare FBG sensor was inserted carefully into the capillary tube. For the isolation of induced strain on the FBG due to the thermal expansion of the capillary tube, one end was left free, and the other end was fixed. After the encapsulation of the sensors inside the stainless steel and borosilicate glass capillary tubes, these tubes were fixed into the wall of the beaker containing water. The sensor was subjected to the temperature change of water from 20 °C to 80 °C at a step interval of 20 °C. We only considered the measurements at three temperatures (20 °C, 40 °C and 60 °C) due to the limitation of controlling the temperature of water in a small interval. The test was repeated several times and the shift in bragg wavelength was averaged to determine the

Table 3
Properties of the Encapsulating Material.

Encapsulated Material	Diameter (Inner/Outer) mm	Thermal Conductivity (W/m-^{0}C) at 25 ^{0}C	Thermal capability(^{0}C)
Borosilicate Glass	0.5/1	1.14	500
Stainless Steel	0.5/1	16	1400

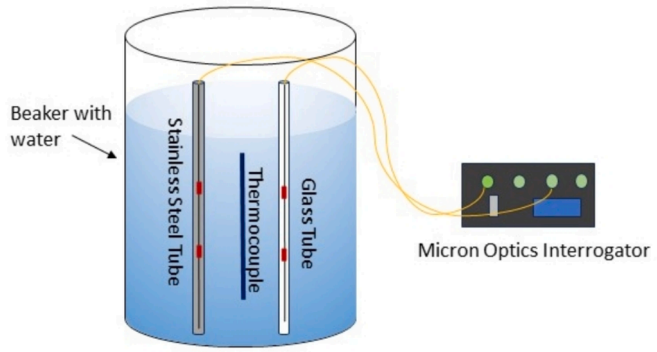

Fig. 2. Schematic diagram of calibration of encapsulated FBG sensor.

sensitivity of the FBG sensors after encapsulation. A thermocouple was also used to monitor the temperature of the water. Both the encapsulated FBG sensors were spliced to the optical patch cord and connected to the Micron Optics Interrogator for data acquisition. Sensors were calibrated considering the temperature as reference parameter, according to the standard practise. This test helped us to determine whether borosilicate glass or stainless steel was the best encapsulation tube for our study.

2.5. Experimental setup

Fig. 3 depicts the experimental setup, adopted to test the reliability of FBG sensors for measuring strain and temperature of the 2CG.

The apparatus is compounded by:

1. Interrogator: Micron Optics Interrogation unit was used for the data acquisition with a sampling frequency of 1 kHz.
2. The dual FBG sensor were used with different bragg wavelengths. One sensor was designed to respond to the strain variations while other was designed more sensitive to the temperature variation. The temperature dual FBG sensor was encapsulated inside a stainless-steel tube.
3. Additional temperature sensor T107 temperature probe was used to compare the temperature measurement with the calibrated stainless-steel tube encapsulated FBG sensors. We also monitored the room temperature using a further thermocouple.

The casting of the four grouts was done according to Todaro and Pace (2022) and the shape of the casting mould was 40 mm*40 mm*160 mm, in compliance to CEN (2016). As depicted in the scheme of Fig. 3 and reported in the photo of Fig. 4 (a), before casting the dual FBG sensors, the stainless steel tube encapsulating the dual FBG sensor, and the temperature sensor (T107-temperature probe) were inserted into the casting mould horizontally through the centre and longitudinally. The bragg wavelength of the dual FBG sensors is summarized in Table 4. The bare FBG sensor was placed directly in contact with the grout and the temperature FBG sensor was isolated from contacting the grout by encapsulating inside a stainless-steel tube. The T107 sensor is a temperature probe used for measuring the temperature of air, water, and soil. It consists of a thermoresistor, encapsulated in an epoxy-filled aluminium housing. This probe was used to compare the temperature measurements from the FBG temperature sensor. These FBG sensors were spliced to the optical patch cord and connected to the micron optics interrogator.

The grouts were prepared based on dosages given in Table 1 and using the bentonites listed in Table 2. After that the components were mixed together, obtained material was quickly poured into the casting moulds as shown in Fig. 4 (b), within the gel time that has order of magnitude of seconds. The casting phase must be completed before the gelation of the material to obtain a homogeneous grout into the mould. Once a sample was casted, the casting surface was scraped with a spatula to obtain a flat surface as depicted in Fig. 4 (b). The scraping phase should be performed within 30–60 s after the casting. Then, the samples were kept in water as shown in Fig. 4 (c) for the rest of the days during the measurement of shrinkage and temperature.

A last test was carried out to study the shrinkage that can potentially occur if the 2CG is cured outside water. The grout prepared using bentonite B1 was selected for this further study and the test had a duration of 5 days.

The described procedure was set-up after a long preliminary pre-trial test campaign performed on only bentonite B1. These tests were necessary in order to calibrate the apparatus, verify the quality of the outcomes, the cable wiring and the curing modality of the samples. As further detail, it is noteworthy to report that the decision to protect the FBG sensors with specific protection tubes was taken due to the need for adopting sufficient energy during the final pouring of the mixed grout in the mould (necessary for complete the casting within the gel-time and to obtain a homogenous sample) and the need for avoid damage on the fibers.

The water used for the sample preparation (as an ingredient) and for the curing was the drinkable water collected from the aqueduct of Turin (Italy). The water does not contain any particular salts and, consequently, it can be considered as a non-aggressive water for the curing.

3. Results

Four different bentonites were tested by using the same mix-design, namely, fixed dosages of each ingredient used for the grout preparation. In this paragraph, after the information related to the temperature calibration, the outcomes of the temperature and shrinkage test campaign are reported. Each grout was independently studied and each experimental chart was inspected to identify some characteristic values. Being constant the mix design, a statistical analysis has been carried out

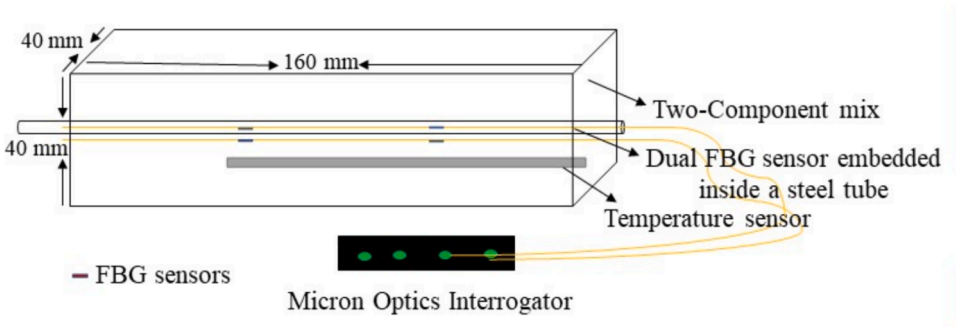

Fig. 3. Schematic diagram of the experimental setup.

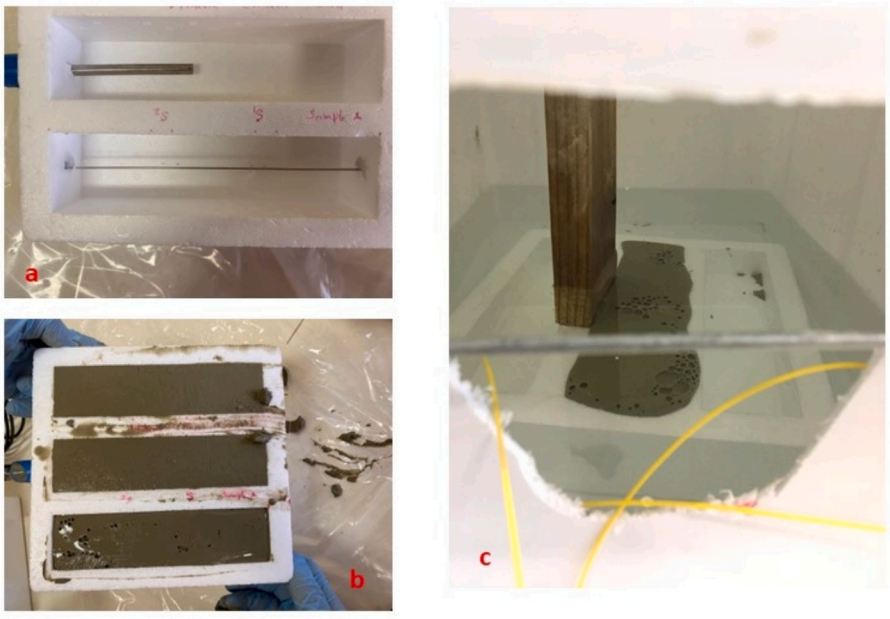

Fig. 4. Preparation of FBG sensor in the casting moulds: (a) before casting, (b) after Casting, (c) sample cured in water.

Table 4
Bragg wavelength of the FBG sensor for different grouts.

Grouts	Bare FBG sensor		Temperature FBG sensor	
	A	B	A	B
B1	1537.924 nm	1545.778 nm	1545.768 nm	1537.876 nm
B2	1537.874 nm	1545.769 nm	1545.779 nm	1537.923 nm
B3	1546.011 nm	1537.893 nm	1538.268 nm	1546.190 nm
B4	1529.808 nm	1537.936 nm	1537.910 nm	1529.837 nm

in order to underline the typical ranges of these characteristic values. As a final analysis, the experimental data from the shrinkage test campaign were interpreted with a curve interpolation in order to provide an experimental law explaining the behaviour of the bentonites.

3.1. Temperature calibration

The parameters that can affect the wavelength shift are the thickness and thermal conductivity of the encapsulated tubes. From Fig. 5 it can be noticed that the stainless-steel encapsulated material provides more shift in bragg wavelength compared to the borosilicate glass with the same thickness. This can be due to the thermal conductivity of stainless steel that is larger than that of the borosilicate glass. The sensor encapsulated inside the stainless-steel tube was used for the measurement of early age temperature change. The estimated thermal sensitivity of stainless steel encapsulating the dual FBG sensor was 11.8 pm/^{o}C.

3.2. Temperature and shrinkage of grouts

3.2.1. Temperature measurement

The temperature measurement of the grout with bentonites B1, B2, B3, and B4 in the 24 h after casting is shown in Fig. 6. The trends for all

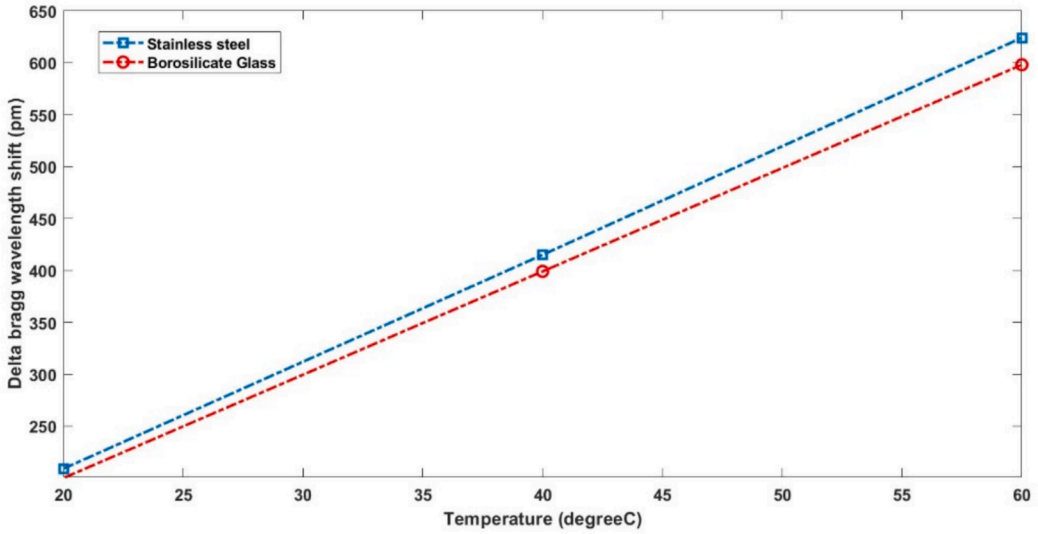

Fig. 5. Temperature response of encapsulated FBG from 20 °C – 60 °C.

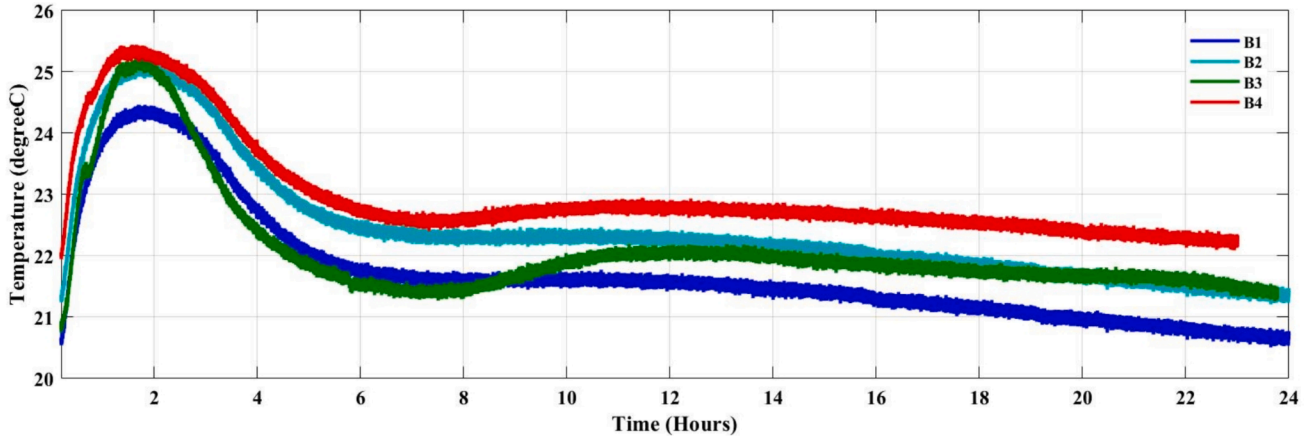

Fig. 6. Temperature measurements of the studied grouts.

grout have almost the same shape.

For each curve, 3 different characteristic values of temperatures were recognised: the maximum reached temperature (T_{max}), the minimum temperature reached after the peak (T_{drop}) and the temperature at the end of the test campaign (T_{24h}). These three characteristic values are highlighted in Fig. 7 for B1.

In Table 5 the characteristic values for temperature are reported. The corresponding time in hours at which T_{max} and T_{drop} were reached is also listed. ΔT_{max} is the maximum difference between the peak temperature T_{max} and T_{24h}. In correspondence of each parameter, the average (Av) and the standard deviation (Std) are indicated.

It should be reported that for grout B3 the parameter T_{24h} actually corresponds to a curing time of 23 h.

3.2.2. *Shrinkage measurement up to 16 days*

The shrinkage measurement was done for 16 days after the casting. The shrinkage plot of the bentonites cured in water is shown in Fig. 8, while Fig. 10 depicts the trend related to the test on bentonite B1 with the curing phase performed outside water, at an average temperature of 21 ± 1 °C (in the range suggested by Wan et al., 2021).

It can be observed from Fig. 8 that the early age shrinkage of grout B1 is more than that of the other grouts. 50 % of the shrinkage happens in the initial hours of casting, while it decreases gradually and remains at a constant value at about 16 days of casting. This marked shrinkage in the initial phase could be correlated to the temperature peak recognised in the first hours of curing, so it can be speculated that the strong shrinkage of the initial phase could be linked to the hydration phenomenon.

Table 5
Characteristic values of temperature for the studied grouts.

	B1	B2	B3	B4	Av	Std
T_{max} (°C)	24.38	25.13	25.30	25.45	25.07	0.41
t (T_{max}) (h)	1.69	1.82	1.72	1.60	1.71	0.08
T_{drop} (°C)	21.54	22.33	21.41	22.50	21.94	0.47
t (T_{drop}) (h)	8.52	7.33	7.45	7.52	7.70	0.47
T_{24h}(°C)	20.65	21.39	21.39	22.24	21.42	0.56
ΔT_{max}	3.73	3.74	3.91	3.21	3.65	0.26

For each curve, two characteristic values of strain have been recognised: the initial shrinkage (ε_{in}), that happened suddenly after the casting, and the final shrinkage (ε_{fin}) at 16 days of curing. These two characteristic values are highlighted in Fig. 9 for B3.

In Table 6 the characteristic values of the shrinkage are reported in με. The difference Δε between the initial and final values of shrinkage is reported. In correspondence of each parameter, the average (Av) and the standard deviation (Sd) are indicated.

As the last step of the work, a further analysis of the shrinkage curves was performed. The data between ε_{in} and ε_{fin} were processed to find the fitting curve that best analytically explained them. The Curve Fitting Toolbox™ in Matlab was used. The best interpolation of the experimental data was the power law with three coefficients:

$$\varepsilon(t) = at^b + c$$

where t is the curing time in days. The coefficients of the equation and

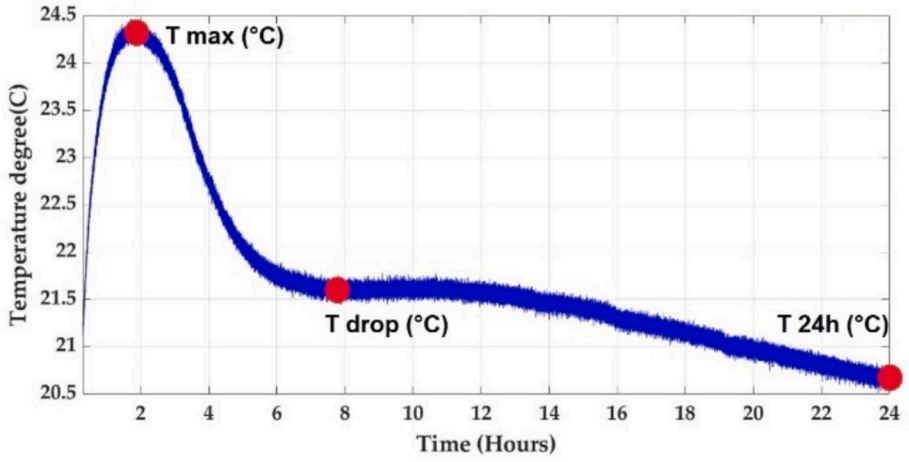

Fig. 7. The three characteristic values of temperature that were picked from the measured charts for each bentonite.

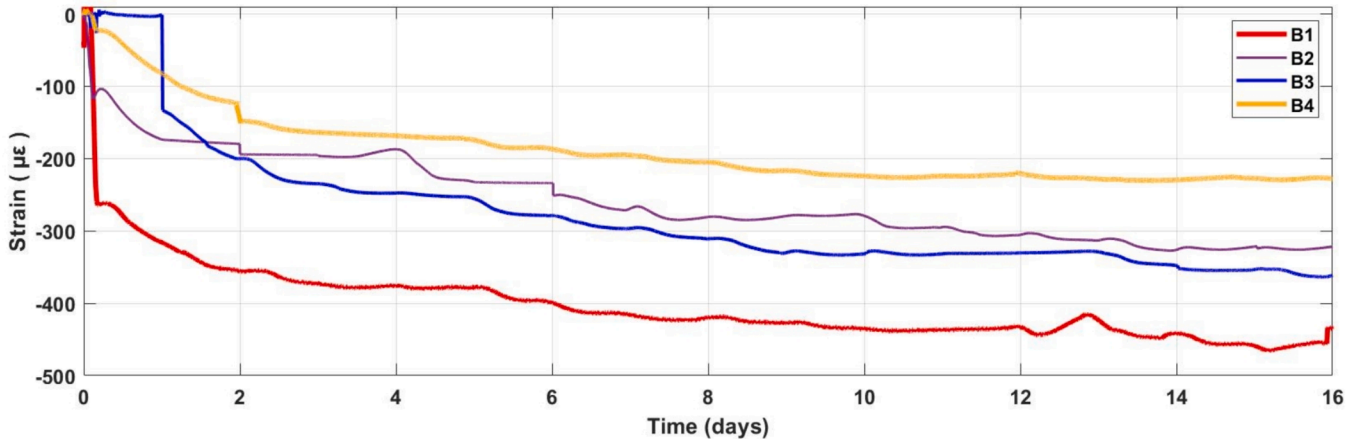

Fig. 8. Early-age shrinkage of the studied grouts.

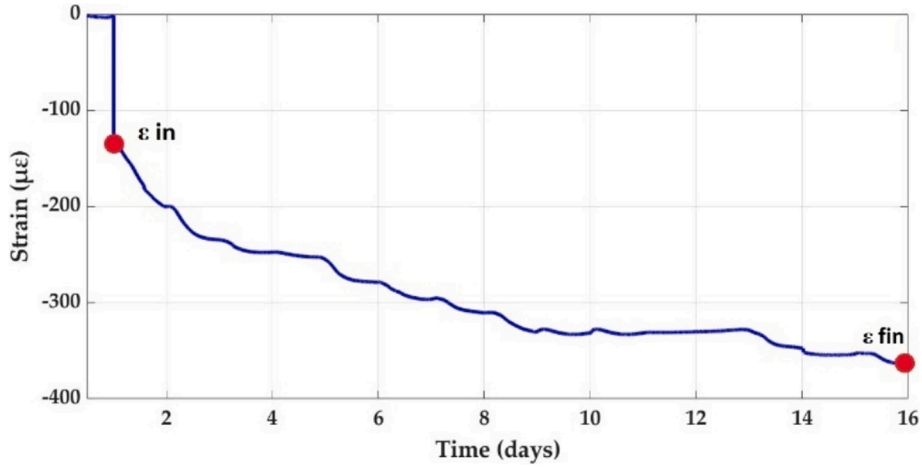

Fig. 9. The two characteristic values of the shrinkage that were picked from the measured charts for each bentonite.

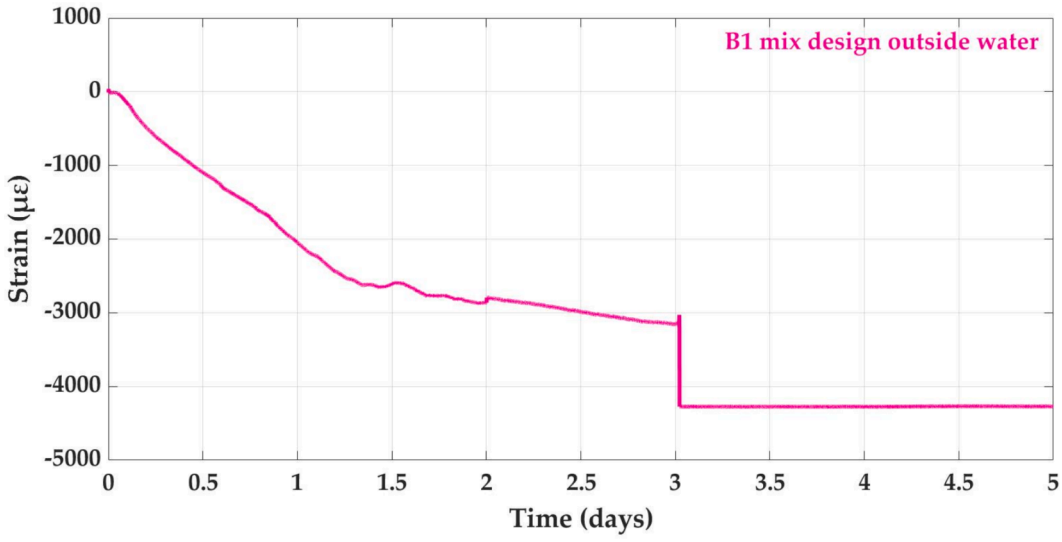

Fig. 10. Early age shrinkage of grout B1 whose curing was outside water.

the R-square of the interpolations are listed in Table 7.

From Fig. 10 it can be noticed that when the sample is not cured in a controlled environmental condition, i.e., if dehydration process is not prevented, an excessive shrinkage occurs, with a consequent fracturing of the sample. The chart reported in Fig. 10 has not been taken into account for statistical analysis since the different curing environment

Table 6
Characteristic values of shrinkage for the studied grouts.

	B1	B2	B3	B4	Av	Std
ε_{in} (με)	−267.14	−118.10	−131.28	−22.09	−134.65	87.33
ε_{fin} (με)	−438.57	−323.81	−364.93	−227.52	−338.71	76.23
Δε (με)	−171.43	−205.71	−233.65	−205.43	−204.05	22.05

Table 7
Coefficients of the power law that interpolates the shrinkage curves for the four two-component grouts. The R^2 of the interpolation is also provided.

Grout	a	b	c	R^2
B1	−96.455	0.291	−232.657	0.995
B2	−51.862	0.541	−100.844	0.968
B3	−423.525	0.143	260.790	0.995
B4	−491.703	0.088	389.728	0.990

completely altered the 2CG behaviour. As concerning the fitting curve, the power law with three coefficients was selected for B1 outside water as well. The obtained equation (a=-2045.200; b=0.451; c=107.902 with R^2=0.976) describes Fig. 10 for the time domain 0–3 days. After 3 days, cracks invaded the sample causing a decoupling between sensors and the body of the sample.

4. Discussion

As concerning the temperature outcomes (Fig. 6) and taking also into account the statistical analysis (Table 5), it can be observed that a positive variation (ΔT_{max}) of almost 4 °C was observed for all the grouts, after the casting of the samples. The maximum temperature (T_{max}) averagely close to 25 °C was reached at about 100 min of curing. The temperature hence dropped to a value ranged between 21.41 and 22.5 °C (T_{drop}) after a curing time that on average is equal to 460 min (7.7 h). It is worth mentioning the low values of standard deviation related to T_{max} and $t(T_{max})$: this low dispersion of results could be strictly correlated to the type and dosage of the used cement. Furthermore, since no strong differences are recognizable also for the other characteristic values of temperatures, it can be speculated that the observed phenomenon is governed by the dosage (w/c ratio) and the type of the used cement (mix design kept constant for all tests). The increasing of the temperature could be consequently correlated to the exothermic reactions between cement, water and accelerator. Hydration is a reaction happening during the setting, which releases heat and results in a sharp increase in the temperature. For long curing times, the temperature of all tested mix designs (T_{24h}) reached 20 ± 2 °C (21.42 °C on average) which was the external air-controlled temperature. It is important to highlight that this trend (i.e., an increase of temperature reaching a peak, followed by a decrease) did not correspond to the trend of the strength. Indeed, if from the one side the curing time of 1.5 – 2 h is the first one that ensure the correct assessment of a uniaxial compression test (Todaro et al., 2020b), on the other side it is well known that the increasing trend in time is continuing fast till 24 h. Consequently, the peaks recognised correspond to specific phases of the hardening process, that in any case continues in time even if the temperature variation becomes no more appreciable by the sensors.

Pertaining to the shrinkage, measurements were performed up to 16 days from the casting. All the tested samples (Fig. 8 and Table 6), irrespective of the used bentonite, were characterised by a strong decrease in the value of strain in the first hours of curing (ε in) which corresponded to a shortening of the samples (negative values of strain correspond to a shortening of the sample). For the test related to bentonite B3, the effective casting of the sample was performed about 40 min later than the beginning of the acquisition of data (the chart is characterised by a short horizontal distribution of data in the first minutes). The chart related to bentonite B4 is different from the others because a strong shortening of the sample was not observed in the first hours of curing (με slowly decreases in time). In fact, after 16 days of curing the maximum value of strain was lower than 250 με, i.e., the lowest value among the tested bentonites. The maximum shrinkage at 16 days of curing was for the grout B1 (about 450 με). The difference in values of shrinkage can be due to the different used bentonites which exhibited different behaviours to face the shrinkage phenomenon to the grout. Unfortunately, it is not possible to correlate the differences found in terms of shrinkage with the bentonite indexes considered in this research (SWI and smectite content). The difficulty in correlating the behaviour of a certain 2CG and the used bentonite is confirmed also in the scientific literature (Todaro and Pace, 2022; Todaro et al., 2023). Globally analysing the results and the common point between the grouts (i.e., the same mix design), it can be stated that the initial value of the shrinkage (ε_{in}) was on average 135 με, while the final value of the shrinkage (ε_{fin}) was instead close to 340 με. The difference between initial and final values (Δε) was instead close to 205 με. Taking into account the standard deviation it can be stated that the dispersion for the characteristic values of the shrinkage was strongly higher than those of the temperature.

A last important consideration is related to the outcomes reported in Fig. 10. The studied sample exhibited a very strong shrinkage phenomenon with values of 3000 με reached after only 3 days of curing. It should be reported that after 3 days of curing the sample was so fractured that the coupling between sensors and the grout was strongly compromised. Consequently, the recording equipment was no more able to continue the correct acquisition of the data. Furthermore, it can be stated that by curing the sample of 2CG outside water, after only 3 days, a shrinkage of about 560 % higher than that obtained after 16 days of curing in water was obtained.

In conclusion, if the curing is performed in a saturated environment, the shrinkage after 16 days of curing is a very limited phenomenon in magnitude (< 500 με), abundantly below the threshold value of 10,000 με reported in the technical specification of some tunnel construction sites (Todaro et al., 2022; Càmara, 2018).

5. Conclusions

The always more complex and detailed numerical models in tunnelling are leading researchers to deeply characterise all the materials involved in a tunnelling construction. The 2CG has recently become one of the most studied materials, since it is crucial to know strains that potentially can occur in this backfilling material, due to the applications of loads or simply due to physiological shrinkage. We investigated the early age shrinkage and temperature of the 2CG. As concerning the shrinkage, the proposed procedure overcomes the limitations typical of the standard concrete procedures since the FBG technology allows the assessment of shrinkage instantaneously after the casting, making the investigation of the short curing time possible (practically impossible with the old standards). The proposed method is currently the only one that allows the assessment of the shrinkage of two-component grouts for curing times lower than 1 day. Indeed, all the standards concerning the shrinkage assessment for common mortars require at least 1 day (or even more than 3 days if the mix-design is not suitable to lock the pins in the body) before reading the “zero” values” (needed for the shrinkage assessment). With the proposed method, the monitoring of the shrinkage begins instantaneously after the casting. Furthermore, the standard regulations permit obtaining only punctual values, while continuous data recording by means of FBG is now allowable. The order of magnitude of the obtained outcomes (hundreds of με after about 2 weeks of curing) is aligned with typical shrinkage data obtained with OS.

Summarising the technical outcomes related to the 2CG, a maximum peak of temperature has been recorded in the first hours of curing, probably due to the exothermic reactions between cement, water and accelerator. This aspect is not a problem in construction sites. Differently, an important aspect has been highlighted concerning the

shrinkage phenomenon: even though a standard 2CG mix exhibits values of shrinkage abundantly within limits reported in technical references, the moisture of the curing environment plays a crucial role. This evidence should be considered in technical specification of construction sites since values of shrinkage could strongly increase if the curing environment has not sufficient moisture content. However, this paper does not cover these types of investigations, as well as no information is available on the effect of shrinkage in the short term on long-term mechanical performances. The authors think that times are too premature for providing an answer to the correlation between early-age properties and long-term performances. These investigations have been however scheduled and results will be available in next future. Furthermore, different test campaigns are also programmed trying to stress the 2CG under different curing environments, more or less aggressive, that will generate positive shrinkage (real shrinkage) or negative shrinkage (expansions of the sample, typical for curing waters containing sulphates). In the light of the results obtained, it is the opinion of the authors that values of shrinkage of 10,000 με reported in technical references could be high, considering that this material could be strongly fractured before reaching these values of shrinkage. Future tests are needed to further investigate this aspect.

As pertaining to the type of bentonite and its effect on the magnitude of the shrinkage, final results cannot be predicted based on the SWI or the content of smectite; it can be speculated that the order of magnitude of the phenomenon could be linked to the mix-design (dosages of ingredients), that is the same for all the test performed. The equations that permit to describe the trend of the shrinkage reported in this work are a useful instrument for improving the knowledge of the phenomenon. However, they should not be used as a prediction tool since values are strictly linked to the mix design and the curing modality (type of water), but for sure they provide an idea of the experimental trend and of the order of magnitude of the phenomenon.

As concerning the FBG technology, the ability of FBG to multiplex, non-destructive, and immune to electromagnetic interface (EMI) is an added advantage of the measurement compared with the conventional sensor. However, for completeness, it is important to report two important obstacles that at the present time constitute a brake to spread this innovative technology. The first is an economic obstacle: the potential limitations of FBG sensors, as they are quasi-distributed sensors, are related to the number of sensors in a fiber since it is limited based on the demodulation technique. The cost of FBG-based systems is higher than that of conventional sensors. It is predictable to reduce the price if industrial sectors that are using the FBG develop the demodulation system according to our needs and multiplexing many sensors. The second obstacle is technical: the sensors are highly fragile and the installation of them should be done with care. Room for improvement may consists in the packaging of the FBG temperature sensors and in the development of the FBG strain sensor instead of the bare sensor for the strain measurement to make the system more rigid and robust.

Fundings

The authors A.G. and A.E. R. are grateful to PhotoNext (competence centre on Applied Photonics of Politecnico di Torino). The research activities carried out in this study were supported and developed in the framework of the centre (50 % funds). This work was also developed at the Department of Environment, Land and Infrastructure Engineering (DIATI) in the frame of the "Department of Excellence" on Climate Transition (2023–2027) (50 % funds). The activity of F. Pace is funded by the NOP Research and Innovation 2014–2020, Axis IV "Education and research for recovery –REACT-EU.

CRediT authorship contribution statement

Aarathy Ezhuthupally Reghuprasad: Writing – original draft, Software, Resources, Investigation, Methodology, Data curation, Formal analysis, Conceptualization. **Carmine Todaro:** Writing – review & editing, Writing – original draft, Resources, Methodology, Investigation, Conceptualization, Visualization. **Francesca Pace:** Data curation, Investigation, Resources, Software, Validation, Visualization, Writing – review & editing. **Daniele Peila:** Writing – review & editing, Supervision. **Alberto Godio:** Writing – review & editing, Supervision, Data curation.

Declaration of competing interest

The authors declare that they have no known competing financial interests or personal relationships that could have appeared to influence the work reported in this paper.

Acknowledgments

The authors want to thank Utt Mapei for having supplied the chemical ingredients and for the given technical support. They also thank Buzzi Unicem for the cement supplied.

Data availability

Data will be made available on request.

References

Càmara, R. J., 2018. Use of two-component mortar in the precast lining backfilling of mechanized tunnels in rock formations, In: ITA WTC Congr. 2018, Dubai (UAE) (2018) 20–26.

CEN., 2002. Products and systems for the protection and repair of concrete structures. Test methods. Determination of shrinkage and expansion. EN EN 12617-4:2002, European Committee for Standardization. Bruxelles (B).

CEN., 2016. Methods of testing cement - part 1: determination of strength. EN 196-1: 2016, European Committee for Standardization. Bruxelles (B).

Dal Negro, E., Boscaro, A., Plescia, E., 2014. Two-component backfill grout system in TBM. The experience of the tunnel 'Sparvo' in Italy, in Proc. TAC Conf. 2014, Vancouver (CA) (2014) 26–28.

Di Giulio, A., Di Felice, M., Valiante, N., De Carli, G., 2023. Single and two-component grout as high-performance backfilling materials. In: Proceedings of the ITA WTC World Tunnel Congress 2023, Athens (EL), May 12–18. 10.1201/9781003348030-147.

EFNARC, 2005. Specification and guidelines for the use of specialist products for Mechanized Tunnelling (TBM) in Soft Ground and Hard Rock, before extraction after extraction. Farnham (UK).

He, S., Lai, J., Wang, L., Wang, K., 2020. A literature review on properties and applications of grouts for shield tunnel. Constr. Build. Mater. 239, 117782. https://doi.org/10.1016/j.conbuildmat.2019.117782.

Jiang, N., Zhu, H., Bao, K., Hu, Y., 2015. Simultaneous discrimination of strain and temperature using dual-gratings in one fiber. Optik (Stuttg) 126 (23), 3974–3977. https://doi.org/10.1016/j.ijleo.2015.07.179.

Kim, J.-K., Lee, C.-S., 1998. Prediction of differential drying shrinkage in concrete. Cem. Concr. Res. 28 (7), 985–994. https://doi.org/10.1016/S0008-8846(98)00077-5.

Luo, D., Ismail, Z., Ibrahim, Z., 2013. Added advantages in using a fiber Bragg grating sensor in the determination of early age setting time for cement pastes. Measurement 46 (10), 4313–4320. https://doi.org/10.1016/j.measurement.2013.06.036.

Mamidi, V.R., Kamineni, S., Ravinuthala, L.N.S.P., Thumu, V., Pachava, V.R., 2014. Characterization of encapsulating materials for Fiber Bragg grating-based temperature sensors. Fiber Integr. Opt. 33 (4), 325–335. https://doi.org/10.1080/01468030.2014.932472.

Mesboua, N., Benyounes, K., Benmounah, A., 2018. Study of the impact of bentonite on the physico-mechanical and flow properties of cement grout. Cogent Eng. 5 (1), 1446252. https://doi.org/10.1080/23311916.2018.1446252.

Oggeri, C., Oreste, P., Spagnoli, G., 2021. The influence of the two-component grout on the behaviour of a segmental lining in tunnelling. Tunn. Undergr. Sp. Technol. 109, 103750. https://doi.org/10.1016/j.tust.2020.103750.

Oreste, P., Sebastiani, D., Spagnoli, G., de Lillis, A., 2021. Analysis of the behavior of the two-component grout around a tunnel segmental lining on the basis of experimental results and analytical approaches. Transp. Geotech. 29, 100570. https://doi.org/10.1016/j.trgeo.2021.100570.

Pei, H., Li, Z., Zhang, B., Ma, H., 2014. Multipoint measurement of early age shrinkage in low w/c ratio mortars by using fiber Bragg gratings. Mater. Lett. 131, 370–372. https://doi.org/10.1016/j.matlet.2014.05.202.

Peila, D., Borio, L., Pelizza, S., 2011. The behaviour of a two-componenet back-filling grout used in a tunnel-boring machine. Acta Geotech. Slovenica 8, 5–15.

Sharghi, M., Chakeri, H., Ozcelik, Y., 2017. Investigation into the effects of two component grout properties on surface settlements. Tunn. Undergr. Space Technol. 63 (2017), 205–216.

Sharghi, M., Chakeri, H., Afshin, H., Ozcelik, Y., 2018. An experimental study of the performance of two-component backfilling grout used behind the segmental lining of a tunnel-boring machine. ASTM Int. J. Test. Eval. 46 (5), 2083–2099. https://doi.org/10.1520/JTE20160617.

Slowik, V., Schlattner, E., Klink, T., 2004. Experimental investigation into early age shrinkage of cement paste by using fibre Bragg gratings. Cem. Concr. Compos. 26 (5), 473–479. https://doi.org/10.1016/S0958-9465(03)00077-5.

Song, W., Zhu, Z., Pu, S., Wan, Y., Huo, W., Song, S., Zhang, J., Yao, K., Hu, L., 2020. Synthesis and characterization of eco-friendly alkali-activated industrial solid waste-based two-component backfilling grouts for shield tunnelling. J. Clean. Prod. 266. https://doi.org/10.1016/j.jclepro.2020.121974. ISSN 0959-6526.

Srimannarayana, K., Shankar, M.S., Prasad, R.L.N.S., Mohan, T.K.K., Ramakrishna, S., Srikanath, G., Rao, S.R.P., 2008. Fiber Bragg grating and long period grating sensor for simultaneous measurement and discrimination of strain and temperature effects. Opt. Appl. 38 (3), 601–608.

Thewes, M., and Budach, C., 2009. Grouting of the annular gap in shield tunneling – an important factor for minimisation of settlements and production performance, In: Proc. ITA-AITES WTC 2009, Budapest (HU), (2009) 23–28.

Todaro, C., Pace, F., 2022. Elastic properties of two-component grouts at short curing times: the role of bentonite. Tunn. Undergr. Sp. Technol. 130, 104756. https://doi.org/10.1016/j.tust.2022.104756.

Todaro, C., Godio, M., Peila, D., 2020a. Ultrasonic measurements for assessing the elastic parameters of two-component grout used in full-face mechanized tunnelling. Tunn. Undergr. Space Technol. 106 (2020), 103630.

Todaro, C., Bongiorno, M., Carigi, A., Martinelli, D., 2020b. Short term strength behavior of two-component backfilling in shield tunneling: comparison between standard penetrometer test results and UCS. Geoing. Ambient. Miner. 159 (1), 33–40.

Todaro, C., Martinelli, D., Boscaro, A., Carigi, A., Saltarin, S., Peila, D., 2022. Characteristics and testing of two-component grout in tunnelling applications. Geomech. Tunn. 15 (1), 121–131. https://doi.org/10.1002/geot.202100019.

Todaro, C., Zanti, D., Carigi, A., Peila, D., 2023. The role of bentonite in two-component grout: a comparative study. Tunn. Undergr. Sp. Technol. 142, 105412. https://doi.org/10.1016/j.tust.2023.105412.

Wan, Y., Zhu, Z., Song, L., Song, S., Zhang, J., Gu, X., Xu, X., 2021. Study on temporary filling material of synchronous grouting in the middle of shield. Constr. Build. Mater. 273, 121681. https://doi.org/10.1016/j.conbuildmat.2020.121681.

Wong, A.C.L., Childs, P.A., Berndt, R., Macken, T., Peng, G.-D., Gowripalan, N., 2007. Simultaneous measurement of shrinkage and temperature of reactive powder concrete at early-age using fibre Bragg grating sensors. Cem. Concr. Compos. 29 (6), 490–497. https://doi.org/10.1016/j.cemconcomp.2007.02.003.

Youn, B., Schulte-Schrepping, C., Breitenbücher, R., 2016. Properties and Requirements of Two-Component Grouts in Mechanized Tunneling, In: ITA WTC WTC Congr. 2016, San Francisco (USA) (2016) 22–28.